



WOODS HOLE OCEANOGRAPHIC INSTITUTION

Applied Ocean Physics and Engineering Department

July 22, 2019

Dr. Scott Harper
Office of Naval Research, Code 322
875 N. Randolph Street
Arlington, VA 22203-1995

Dear Dr. Harper:

Enclosed is the Final Report for ONR Grant No. N00014-16-1-2486 entitled "Formation of Dunes on the Upper Slope by Internal Solitary Waves in the South China Sea," Principal Investigators, Drs. John Trowbridge and Benjamin Reeder.

Sincerely,

Shirley Barkley

Shirley Barkley
Administrative Associate II

Enclosure

cc: Administrative Grants Officer
AOPE Department Office (WHOI)
✓ Defense Technical Information Center
Naval Research Laboratory

Final Report

Formation of Dunes on the Upper Slope by Internal Solitary Waves in the South China Sea

22 July 2019

John Trowbridge
Applied Ocean Physics & Engineering Department
Woods Hole Oceanographic Institution
Losos 204; MS # 57
Woods Hole, MA 02543
phone: 508-289-2296 email: jtrowbridge@whoi.edu

D. Benjamin Reeder
Department of Oceanography
Graduate School of Engineering and Applied Sciences
Naval Postgraduate School
Monterey, CA 93943
Email: dbreeder@nps.edu

Award Number: N00014-16-1-2486

Major Goals

Reeder et al (2011) discovered large sand dunes, with lengths of approximately 300 m and heights up to 16 m, on the upper slope in the South China Sea (Figure 1), the site of the world's largest observed internal solitary waves (ISW; Ramp et al. 2006, Chao et al. 2007, Shaw et al. 2009; Figure 2). The dunes, unique in their slope location and possible formation by ISW, are of interest intrinsically and because similar seafloor features in other locations are known to refract and focus low-frequency sound (Ballard et al 2012). The processes that form the dunes and determine their occurrence and scales have not been determined.

Reeder et al. (2011) hypothesized that the internal waves form the dunes, citing observations (Bogucki et al 1997, 2005; Bogucki & Redekopp 1999, Klymak & Moum 2003), simulations (Diamessis & Redekopp 2006), and experiments (Carr et al 2008) that indicate enhanced turbulence and sediment resuspension in internal wave wakes. However, a mechanism by which the internal solitary waves might form the dunes has not been proposed, and a dynamical framework for predicting the occurrence and scales of the dunes does not exist.

The overall goals of the project were to:

- Test the hypothesis that the sand dunes that have been observed on the upper slope in the South China Sea are formed by the observed internal solitary waves.
- Obtain a quantitative understanding of the processes the form the dunes.
- Develop a quantitative ability to predict the occurrence and scale of the dunes.

Accomplishments

Analysis of existing measurements

The existing echo-sounder measurements, obtained by Reeder and colleagues in 2007, quantified one wave as it propagated over the dune field, between water depths of approximately 600 m and 150 m (Figure 3). Conductivity-temperature-depth (CTD) measurements at four locations accompanied the echo-sounder measurements. The analysis focused on testing consistency of the wave shapes and phase speeds with the ISW solution of the Korteweg-de Vries (KdV) equation (e.g. Grimshaw et al. 2004, Helfrich & Melville 2006), evaluating an energy balance, and testing the relationship between the observed wavelength of the sand dunes and two length scales that characterize the ISW: the wavelength and the particle excursion $\int U dt$, where U is the near-bottom velocity and t is the time.

The analysis indicates close consistency of the observed wave shapes with the ISW solution to the KdV equation (Figure 4, top panel) and approximate consistency between observed phase speeds and computations based on linear and nonlinear theory (Figure 4, bottom panel). The results indicate a loss of approximately 80% of the ISW energy $\int E dx$, where E is the energy density and x is the along-propagation coordinate, at water depths between 600 m and 350 m (Figure 5, top panel), coincident with the dune field (Figure 1). The analysis indicates that the observed dune wavelength is much smaller than the ISW wavelength and nearly equal to the particle excursion $\int U dt$ (Figure 5, bottom panel), where U is calculated from the observations using linear theory with the observed density structure. The loss of energy is larger than can be explained by either a conventional bottom drag law or interfacial mixing, given estimates of Richardson numbers based on the measured stratification and velocity gradients estimated from linear theory.

Comparison of existing observations with Korteweg-de Vries theory (with Karl Helfrich, WHOI)

To complement the analysis of the Reeder et al. (2011) observations discussed above, we have undertaken a modeling effort based on the variable-coefficient Korteweg-de Vries (KdV) theory (c.f. Grimshaw et al., 2004). The KdV model is set-up to replicate the observation section using the bottom topography from Figure 1 and the mean stratification obtained by Reeder et al. The horizontal length scale of the same dunes, comparable with the water depth, is too short for the assumptions inherent in the KdV theory, so the dunes have been filtered out. We make the assumption that for the evolution of the solitary waves, the dunes are primarily responsible for an enhanced bottom drag, or boundary layer dissipation. The effect is parameterized in the KdV model through a quadratic drag formulation with a spatially variable drag coefficient $C_d(x)$. Then we adjust $C_d(x)$ to obtain the best fit with the observations.

Figure 6 show the results from a KdV run initialized with a mode-one KdV solitary wave of depression with amplitude $\eta_0 = -145$ m in water of depth $h = 582$ m. The model calculation shows that the solitary wave evolves essentially adiabatically, remaining as a single solitary wave that adjusts slowly to the changing depth and bottom drag, with little evidence of topographic scattering until the wave reaches a depth of about 200 m ($x = 38$ km in the figure). This supports the interpretation of the acoustic observations (Figure 3) and analysis in Figure 5.

The best fit to the observations of wave amplitude and energy is obtained with an elevated quadratic drag coefficient $C_d = 0.06$ for water depths h greater than ≈ 400 m and $C_d = 0.001$ for shallower depths (used in Figure 6). A comparison of the observations and the results from the KdV model for this C_d spatial structure is shown in Figure 7. The agreement between the observations and KdV theory is very good and lends support to the hypothesis that the principal effect of the large-amplitude dune field, found for $h > 350\text{-}400$, is to cause enhanced dissipation of internal solitary waves. It remains to understand the local boundary layer flow dynamics above dunes that results in the enhanced drag.

Analysis of the stability of an erodible seabed beneath internal solitary waves

The analysis addresses a configuration (Figure 8) in which the ISW form a turbulent bottom boundary that interacts with perturbations in the elevation of the erodible seafloor. The analysis indicates dune growth when there is convergence of sediment flux over the dune crests and a divergence over the dune troughs. The analysis is based on standard boundary layer theory, similar to the analysis of airflow over water waves (e.g. Janssen 2004) and existing bedload and suspended sediment transport formulas (e.g. Fredsoe & Deigaard 1994). The analysis produces a most unstable dune wavelength, which can be compared with observations, and the growth rates of the dunes.

The analysis indicates dune wavelengths comparable to the particle excursion JU_{dt} , consistent with the observations (Figure 5, bottom panel). Both suspended and bedload transport are required to produce the observed wavelength. The analysis indicates long timescales for dune growth (many centuries).

New measurements over the dune field

The new measurements were motivated by results presented at a Project Meeting at the National Taiwan University (NTU) in Taipei in October 2016. The measurements were funded and executed by the Taiwanese under the leadership of NTU Professor Y. J. Yang, with the participation of the US PIs (Trowbridge and Reeder).

The Taiwanese research vessel OR3 departed Kaohsiung on 25 May 2017. Moorings were deployed at two depths (500 m and 400 m) to determine the temperature and velocity structure throughout the water column and the near-bottom turbulence characteristics (Figure 9). Shipboard echo-sounder measurements (similar to Figure 3) quantified the shapes and phase speeds of the ISW. Shipboard CTD measurements determined the density structure and the relationship between temperature and density (for interpretation of the moored temperature measurements). The moorings were recovered and the ship returned to port on 29 May 2017. Analysis of the measurements is ongoing.

Dissemination

Nothing to report. However, this effort continues through a new ONR grant N00014-18-1-2542 (5/1/2018-5/31/2020) titled "Formation of Sand Dunes by Internal Solitary Waves in the South China Sea," K. Helfrich and J. Trowbridge, co-PIs. The new ONR grant will result in publications describing the

References

- Ballard, M. S., Lin, Y. T., Lynch, J. F. 2012. Horizontal refraction of propagating sound due to seafloor scours over a range-dependent layered bottom on the New Jersey shelf. *Journal of the Acoustical Society of America* 131, 2587-2598.
- Bogucki, D., Dickey, T., Redekopp, L.G., 1997. Sediment resuspension and mixing by resonantly generated internal solitary waves. *Journal of Physical Oceanography* 27, 1181–1196.
- Bogucki, D.J., Redekopp, L.G. 1999. A mechanism for sediment resuspension by internal solitary waves. *Geophysical Research Letters* 26, 1317–1320.
- Bogucki, D.J., Redekopp, L.G., Barth, J. 2005. Internal solitary waves in the coastal mixing and optics 1996 experiment: multimodal structure and resuspension. *Journal of Geophysical Research* 110, C02023.
- Carr, M., Davies, P.A., Shivaram, P. 2008. Experimental evidence of internal solitary wave-induced global instability in shallow water benthic boundary layers. *Physics of Fluids* 20 (066603), 1–12.
- Chao, S.-Y., Ko, D.-S., Lien, R.-C., Shaw, P.-T., 2007. Assessing the west ridge of Luzon Strait as an internal wave mediator. *Journal of Oceanography* 63, 897–911.
- Fredsoe, J., Deigaard, R. 1994. *Mechanics of Coastal Sediment Transport*. World Scientific.
- Diamessis, P.J., Redekopp, L.G. 2006. Numerical investigation of solitary internal wave induced global instability in shallow water benthic boundary layers. *Journal of Physical Oceanography* 36, 784–812.
- Grimshaw, R., Pelinovsky, E., Talipova, T., Kurkin, A. 2004. Simulation of the transformation of internal solitary waves on oceanic shelves. *Journal of Physical Oceanography* 34, 2774-2791.
- Helfrich, K. R., Melville, W. K. 2006. Long nonlinear internal waves. *Annual Review of Fluid Mechanics*. 38, 395-425. DOI: 10.1146/annurev.fluid.38.050304.092129.
- Janssen, P. 2004. *The Interaction of Ocean Waves and Wind*. Cambridge University Press.
- Klymak, J.M., Moum, J.N. 2003. Internal solitary waves of elevation advancing on a shoaling shelf. *Geophysical Research Letters* 30 (20), 2045.
- Ramp, S.R., Chiu, C.-S., Bahr, F.L., Tang, T., Yang, Y. 2006. Characterizing the internal wave field in the Northeastern South China Sea. *EOS. Transactions of the American Geophysical Union* 87 (36) (Ocean Sciences Meeting Supplement, Abstract OS11J-01).
- Reeder, D. B., Ma, B. B., Yang, Y. J. 2011. Very large subaqueous sand dunes on the upper continental slope in the South China Sea generated by episodic, shoaling deep-water internal solitary waves. *Marine Geology* 279, 12-18.

Shaw, P.-T., Ko, D.S., Chao, S.-Y., 2009. Internal solitary waves induced by flow over a ridge: with applications to northern South China Sea. *Journal of Geophysical Research* 114, C02019. doi:10.1029/2008JC005007.

Figures

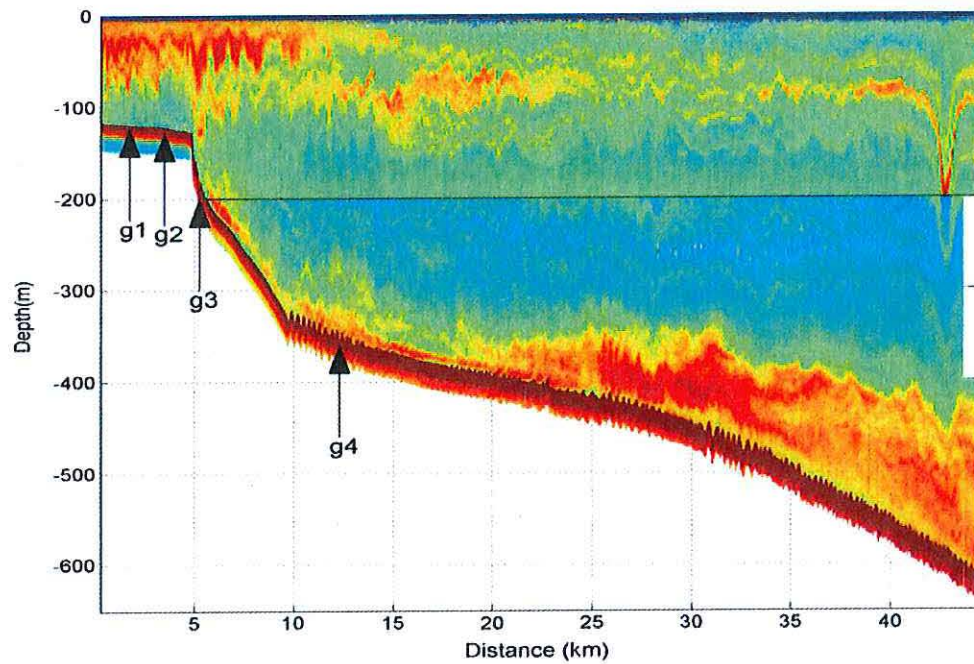


Figure 1. Imagery from Reeder et al. (2011) showing dunes of length approximately 300 m and height up to 15 m (between water depths of approximately 350 and 600 m), a scattering layer at a depth of approximately 100 m, and an onshore-propagating internal solitary wave with an amplitude of approximately 125 m.

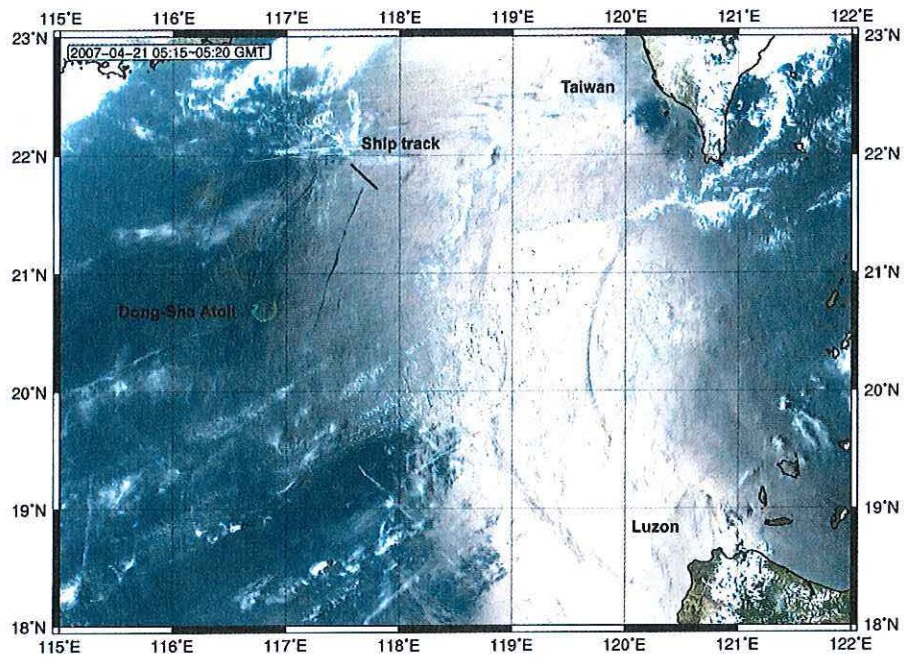


Figure 2. Satellite imagery showing Taiwan, Luzon, and the South China Sea. The generation region for internal solitary waves is Luzon Strait, between Taiwan and Luzon. The image shows a large internal solitary wave near 120°E between 20° and 21°N, and a smaller internal solitary wave near 117.5°E between 20.5°N and 21.5°N. The ship track shows the location of the measurements in Figure 1. Figure reproduced from Reeder et al. (2011).

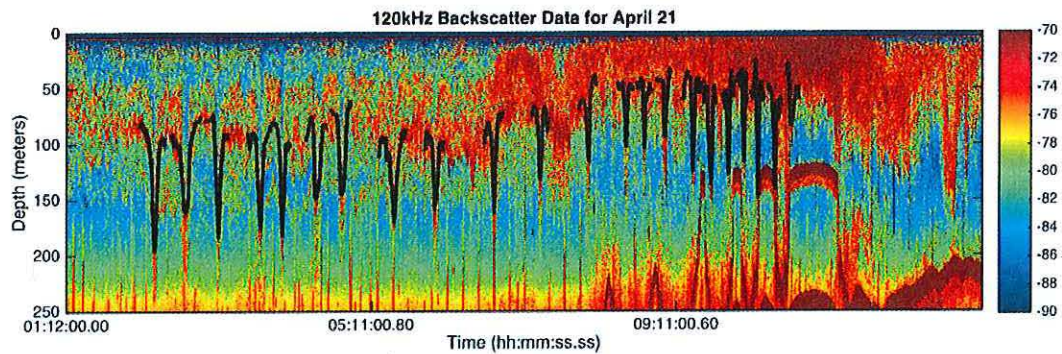


Figure 3. Composite summary of the echo-sounder imagery of internal solitary waves obtained by Reeder and colleagues at the study site (Figure 1) in 2007. The measurements were obtained over a period of approximately eight hours. The imagery shows the displacement of a layer occupied by acoustic scatterers as the wave propagated shoreward (to the right in this image).

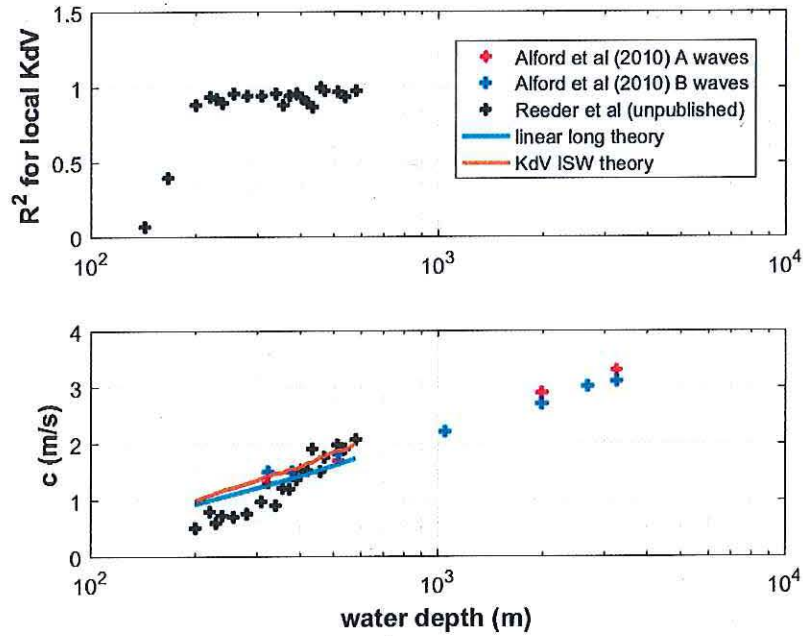


Figure 4. Squared correlation coefficient R^2 for fits of the observed wave shapes with the ISW solution to the KdV equation (top panel) and comparisons of the observed propagation speed c with calculations based on linear and nonlinear theory (bottom panel). In addition to the measurements by Reeder and colleagues, measurements in deeper water from Alford et al. (2010), at a site with similar characteristics but located approximately 100 km to the northwest, are included for the purposes of comparison.

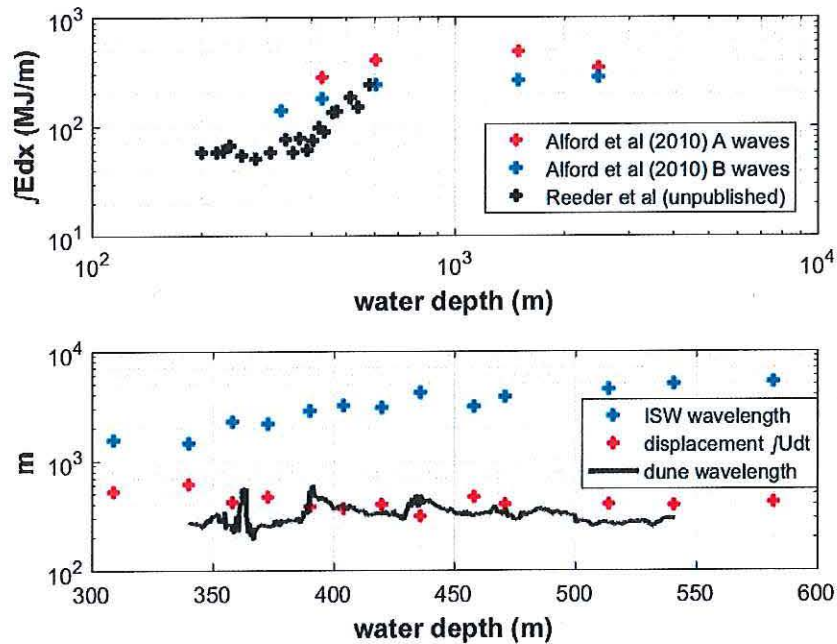


Figure 5. Spatial integrated energy density $\int E dx$ as a function of water depth (top panel) and a comparison of the ISW wavelength, the ISW-induced displacement $\int U dt$, and the observed dune wavelength, all as functions of the water depth (bottom panel).

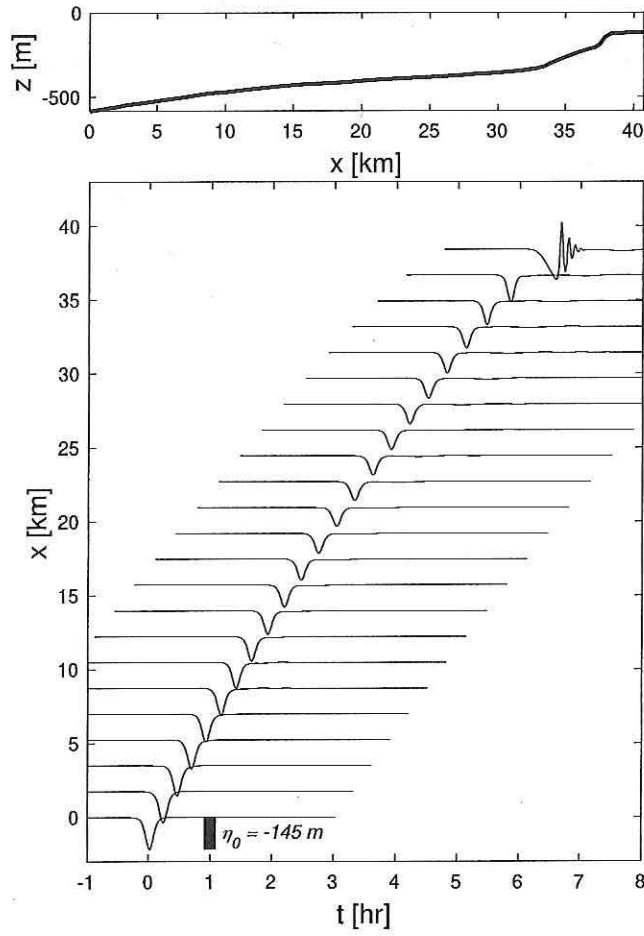


Figure 6. Results from a numerical solution to the variable coefficient KdV equation for an internal solitary wave with initial amplitude $\eta_0 = -145$ m in $h = 582$ m of water propagating inshore. The topography (absent the same dunes) and stratification used to calculate the KdV equation coefficients are from the Reeder et al. (2011) observation site. The top panel shows the topography where $h = 600$ m. The bottom panel shows time series of wave amplitude $\eta(x, t)$ at x -locations indicated by the vertical axis. The calculations were made with a bottom quadratic drag coefficient $C_d = 0.06$ for depths $h \geq 400$ m and $C_d = 0.001$ for depths $h < 400$ m to obtain the best fit with the observations (see Figure 7).

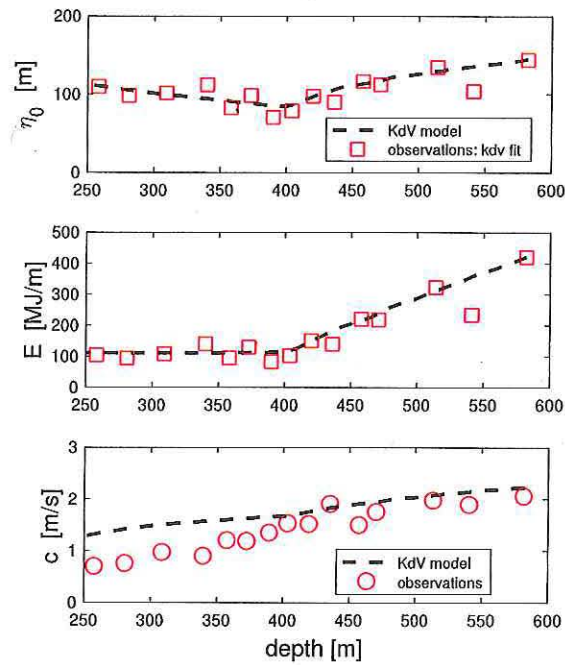


Figure 7. Comparison of the Reeder et al. (2011) observations with results from the KdV solution in Figure 6. The figure shows solitary wave amplitude η_0 (top panel), integrated solitary wave energy E (middle), and phase speed c (bottom) versus the local water depth.

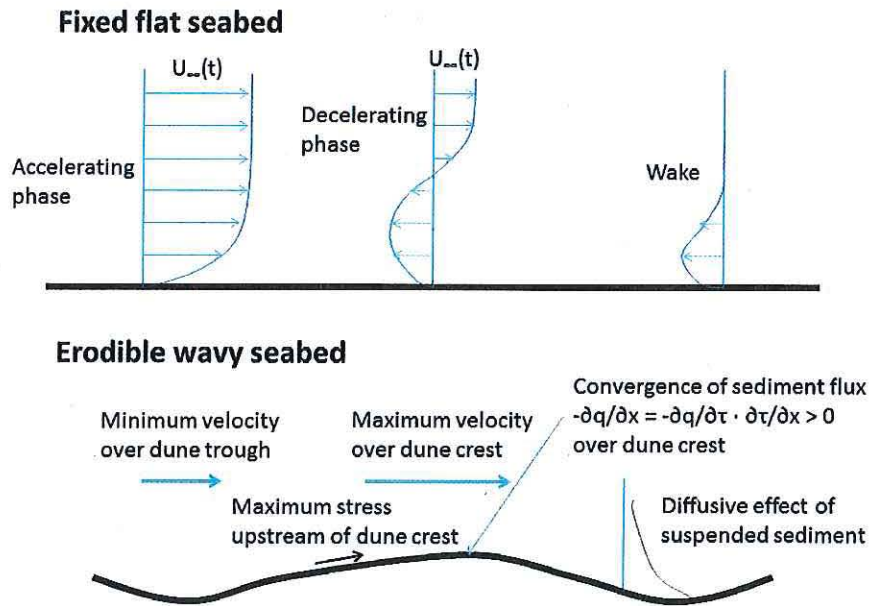


Figure 8. Schematic diagram showing the framework for the linear analysis of the stability of an erodible sandy seabed beneath the turbulent boundary layer formed by an internal solitary wave. The internal solitary wave is propagating to the left. Conservation of mass dictates that the flow near the bottom is to the right. The top panel shows the boundary layer structure over a fixed flat seabed. The bottom panel shows the velocity, stress and sediment patterns over a wavy seabed.

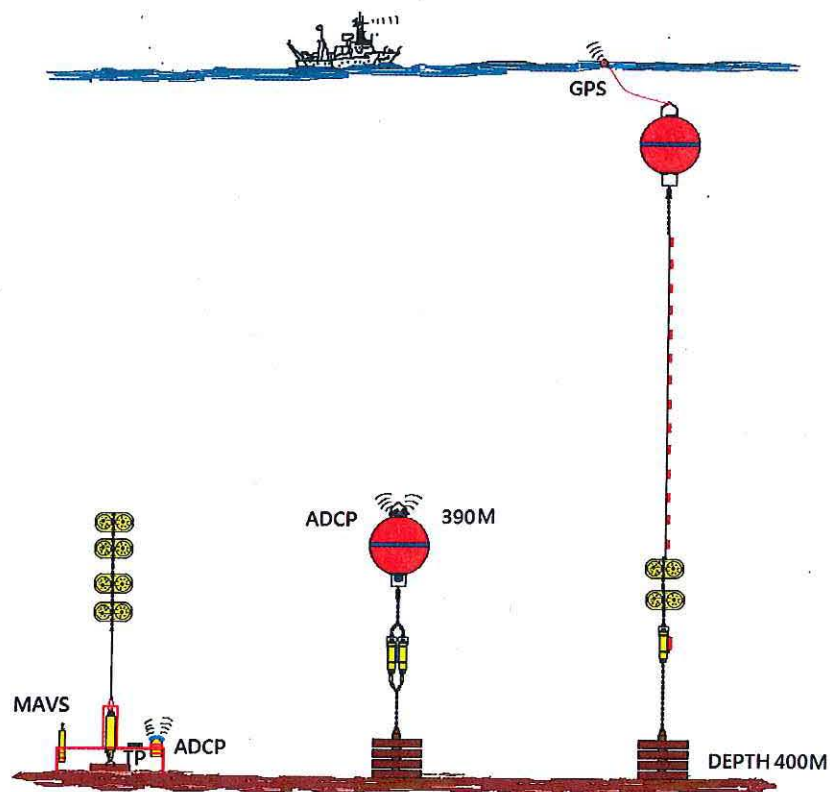


Figure 9. Schematic of moorings deployed at a depth of 400 m. A bottom frame with buoyancy and an acoustic release (far left) supported a point velocity sensor for turbulence measurements (MAVS) and an upward looking high-frequency acoustic Doppler current profiler (ADCP) for near-bottom velocity measurements. A mooring with an acoustic release and subsurface buoyancy (center) supported an upward-looking ADCP to measure currents throughout the water column. A mooring with a release and subsurface buoyancy (far right) supported multiple temperature sensors. The array at 500 m was similar.

REPORT DOCUMENTATION PAGE

Form Approved
OMB No. 0704-0188

The public reporting burden for this collection of information is estimated to average 1 hour per response, including the time for reviewing instructions, searching existing data sources, gathering and maintaining the data needed, and completing and reviewing the collection of information. Send comments regarding this burden estimate or any other aspect of this collection of information, including suggestions for reducing the burden, to Department of Defense, Washington Headquarters Services, Directorate for Information Operations and Reports (0704-0188), 1215 Jefferson Davis Highway, Suite 1204, Arlington, VA 22202-4302. Respondents should be aware that notwithstanding any other provision of law, no person shall be subject to any penalty for failing to comply with a collection of information if it does not display a currently valid OMB control number.

PLEASE DO NOT RETURN YOUR FORM TO THE ABOVE ADDRESS.

1. REPORT DATE (DD-MM-YYYY) 07/22/2019			2. REPORT TYPE Final Report		3. DATES COVERED (From - To) 05/01/2016 - 4/30/2019	
4. TITLE AND SUBTITLE Formation of Dunes on the Upper Slope by Internal Solitary Waves in the South China Sea					5a. CONTRACT NUMBER	
					5b. GRANT NUMBER N00014-16-1-2486	
					5c. PROGRAM ELEMENT NUMBER	
6. AUTHOR(S) Dr. John Trowbridge and Dr. D. Benjamin Reeder					5d. PROJECT NUMBER	
					5e. TASK NUMBER	
					5f. WORK UNIT NUMBER	
7. PERFORMING ORGANIZATION NAME(S) AND ADDRESS(ES) Applied Ocean Physics & Engineering Department Woods Hole Oceanographic Institution 266 Woods Hole Road Woods Hole, MA 02543-1536					8. PERFORMING ORGANIZATION REPORT NUMBER	
9. SPONSORING/MONITORING AGENCY NAME(S) AND ADDRESS(ES)					10. SPONSOR/MONITOR'S ACRONYM(S)	
					11. SPONSOR/MONITOR'S REPORT NUMBER(S)	
12. DISTRIBUTION/AVAILABILITY STATEMENT Approved for public release; distribution is unlimited						
13. SUPPLEMENTARY NOTES						
14. ABSTRACT see attached report.						
15. SUBJECT TERMS Internal waves, sand dunes, South China Sea						
16. SECURITY CLASSIFICATION OF:			17. LIMITATION OF ABSTRACT	18. NUMBER OF PAGES	19a. NAME OF RESPONSIBLE PERSON	
a. REPORT	b. ABSTRACT	c. THIS PAGE			Dr. John Trowbridge	
UL	UL	UL	UL	10	19b. TELEPHONE NUMBER (Include area code) 508-289-2296	